

# An Integrated Time-Varying Ornstein-Uhlenbeck Process for Jointly Modeling Individual and Population-Level Dynamics of Golden Eagles

Michael L. Shull<sup>\*a</sup>, Ephraim M. Hanks<sup>a</sup>, James C. Russell<sup>b</sup>, Robert K.  
Murphy<sup>c</sup>, and Frances E. Buderman<sup>d</sup>

<sup>a</sup>Department of Statistics, The Pennsylvania State University, University  
Park, PA, USA

<sup>b</sup>Department of Mathematics, Computer Science, and Statistics,  
Muhlenberg College, Allentown, PA, USA

<sup>c</sup>Eagle Environmental Inc., Santa Fe, New Mexico, USA

<sup>d</sup>Department of Ecosystem Science and Management, The Pennsylvania  
State University, University Park, PA, USA

## Abstract

With technological advancements, the quantity and quality of animal movement data has increased greatly. Currently, there is no existing movement model that can be used to describe full year of migratory species data that leverages both individual movement data and species distribution data. Herein we propose a full-year stochastic

---

<sup>\*</sup>Corresponding author - email: mlshull@psu.edu

differential equation model for jointly modeling both individual movement data and species distribution data. We show that this joint model, under certain assumptions, results in efficient computation of the spatio-temporal dynamics of the entire population, and thus provides straightforward inference on the species distribution data. We illustrate this model with 215 bird-years of golden eagle movement in western North America and data from eBird for the species distribution.

Keywords: ecology, animal movement modeling, Bayesian statistics, migratory birds, GPS data

## 1 Introduction

Managing migratory species is challenging as it requires an understanding of spatio-temporal migration patterns, which can span nations and even continents. This understanding gives us the ability to estimate potential effects of climate and land-use change have on migratory species. One example would be the evaluation of risk that wind energy projects pose to migratory birds such as golden eagles (*Aquila chrysaetos*) (Beston et al., 2016). In the western U.S., golden eagle mortality due to collisions with wind turbines, specifically with spinning turbine blades (Hunt, 2002; Hunt and Watson, 2016), has increased steadily and may be having population-level effects (Gedir et al., 2025). Government and private entities who perform environmental impact studies are interested in the spatio-temporal distribution of eagles that would be negatively impacted by the construction of a wind project in a certain location as well as understanding the relative risks posed by existing wind projects. Another example is managing game species such as mallard ducks (*Anas platyrhynchos*). Summer breeding grounds and winter ranges are often thousands of miles apart for mallards; therefore, government agencies that manage breeding grounds must work together with those that manage winter ranges to successfully maintain mallard populations (U.S. Department of the Interior, 2024). Models that capture the spatio-temporal dynamics of migratory species for the full-annual cycle are essential for principled management of migratory species like

mallards and golden eagles..

One means of collecting movement data from migratory species is placing GPS trackers on individuals in the population. GPS data provide us with time-indexed spatial information on how individuals in the population of interest move during both migratory and non-migratory seasons. However, these data do not provide unbiased information regarding the spatio-temporal distribution of the entire population, as these samples are almost never representative of the entire population of interest (Gow et al., 2019; Hertel et al., 2020; Norevik et al., 2025).

An additional source of movement data for migratory species comes from citizen science initiatives. For example, birdwatchers can report geo-referenced auditory or visual detections of individual birds to the eBird platform; although some detected birds may be marked with bands or GPS trackers, the majority are unmarked. These records can then be used to produce estimates of the spatio-temporal distribution for a given species at a fine spatial resolution (Fink et al., 2013). This aggregated data product can give great insight into the spatio-temporal dynamics of a migratory species; however, this population-level data source provides no insight into individual migration patterns.

In this paper we build a joint full-annual cycle model for these two data streams, which allows us to leverage individual migration patterns from GPS tracking data with information from citizen science data about the spatio-temporal distribution of the species to estimate full annual-cycle migratory dynamics and assess the varying spatial risk from hazards to different subsets of the population during both migratory and non-migratory seasons. One recent approach of jointly modeling these two types of data is the Integrated Movement Modeling (IMM) framework of Buderman et al. (2025). This method integrates a statistical model for individual tracking data over a model for the heterogeneity of movement behavior within a population to obtain a probabilistic model for the spatio-temporal dynamics of the species' population. Buderman et al. (2025) illustrate this framework in modeling golden eagle migration in western North America. However, they restrict their analysis to 8 weeks of the

spring migration, pre-divide the individual tracking data into two groups based on maximum latitude achieved during spring, and use a numerical approximation to their movement model for individual tracking data.

In this paper, we improve the IMM framework of Buderman et al. (2025) to address questions related to full annual cycle dynamics of migratory species, such as the risk wind projects pose to golden eagles in Western North America. In contrast to Buderman et al. (2025), we consider the full annual cycle rather than modeling the spring migration. While Buderman et al. (2025) used a numerical approximation to a stochastic differential equation (SDE) model for individual tracking data, we develop a time-varying Ornstein-Uhlenbeck (OU) model for animal movement, scale it up to derive a formal probabilistic model for the spatio-temporal population dynamics, and show that this SDE has an analytic solution that makes computing and inference very efficient, even for continental-scale inference.

The novel, time-varying OU process model we propose allows us to answer both population and individual-level questions about golden eagle movement behaviors. We use this model to examine how migration timing varies among different individual eagles in the population as well as to assess wind project risks for golden eagles that winter in specific locations.

## 2 Data

We obtained movement data from 93 golden eagles tracked by the U.S. Fish and Wildlife Service (USFWS) via GPS satellite telemetry during 2011-2018; individual eagles in our sample were represented by data from one to six complete years each. We treated each year of data from an eagle as being independent of all other years of data for that individual (hereafter, each will be referred to as a bird year). In total we have 215 bird years worth of data. Eagles were tagged in the Colorado Plateau, Rocky Mountain (south of Montana), Central Great Plains, Southern Great Plains, and Texas Trans-Pecos regions, encompassing roughly the eastern one-half of the species' range in the coterminous western U.S. Most

(77.9%) were tagged with satellite transmitters when they were large (7- to 8-week old) nestlings; these permanently dispersed from natal areas by the end of their first year of life (Murphy et al., 2017). Others (22.1%) were trapped and tagged when in their second year of life or older; including some that were settled on breeding territories when four years of age or older (Murphy et al., 2019). Transmitters were solar Argos/GPS 45-g and 70-g platform terminal transmitter units (Microwave Telemetry, Inc., Columbia, MD); each was attached in a backpack configuration via a “Y-harness” constructed of Teflon ribbon (Murphy et al., 2017). Transmitters collected GPS locations hourly each day during at least 0900-1600 H; PTT location accuracy was  $\pm 19$  m (Murphy et al., 2017). Our dataset for a given eagle included a single daily location for each 24-hour period, derived by averaging all GPS locations available for the 24-hour period.

As we describe in Section 3.2, heterogeneity in movement behavior will be modeled via a mixture model. This is heuristically equivalent to the population being composed of several sub-populations. We clustered the telemetry data into four groups using the k-means algorithm (Steinley, 2006). We assumed that eagles in these four sub-populations would differ in their geographic centroids, attraction to their respective centroids, and migration timing (these three characteristics comprise the parameters in our selected movement model); however, any quantities within a defined movement model could be used to subdivide a population. This procedure resulted in 11, 13, 24, and 167 bird-years in each sub-population respectively. Figure 1 shows the telemetry data divided by sub-population. These four sub-populations could be described as moderate-distance migrants, long-distance migrants, short-distance migrants, and non-migratory (full-year resident) eagles respectively.

For species distribution data, we use eBird relative abundance data. The Cornell Lab of Ornithology has developed the Adaptive Spatio-Temporal Exploratory Model, adaSTEM, (Fink et al., 2013, 2014), which processes huge numbers of individual citizen-science records and accounts for spatial heterogeneity in sampling effort, observer skill, and rarity of species to estimate the relative abundance of a species over space and time (Fink et al., 2013).

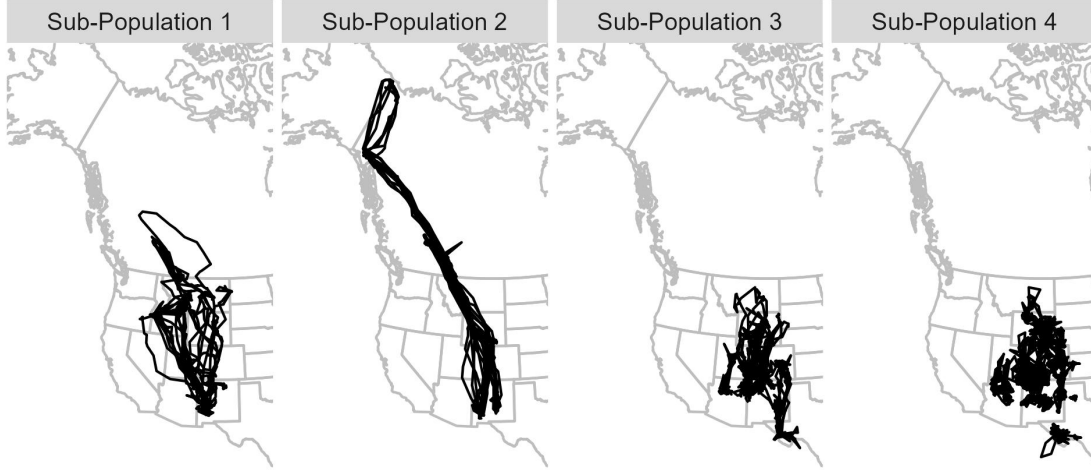


Figure 1: Movement tracks based on satellite telemetry data for golden eagles in western North America, separated by sub-population. The eagles were placed in sub-populations based on a clustering of their full annual telemetry dataset via k-means algorithm. This highlights the different migratory behaviors that individual golden eagles exhibit. These four sub-populations could be described as moderate-distance migrants, long-distance migrants, short-distance migrants, and non-migratory (full-year resident) eagles respectively.

Several studies have shown that relative abundances produced by the adaSTEM models accurately represent avian spatial distributions (Ruiz-Gutierrez et al., 2021; Howell et al., 2022; Stuber et al., 2022; Stillman et al., 2023). This eBird relative abundance information is available at a 2.8 x 2.8km resolution, at weekly intervals through a given year, throughout the golden eagles' range.

We subset the 2019 relative abundance (Fink et al., 2021) down to western North America, aggregated to 100-km resolution, and normalized the gridded relative abundance to sum to unity for each time point. We used this weekly, normalized, eBird relative abundance as the species distribution data in our analysis. Figure 2 presents these data for selected weeks, showing the variable nature of golden eagle migration in western North America, with some of the population migrating south in fall from Alaska and northwestern Canada

to far southwestern Canada and the contiguous western US then returning north in spring, some remaining year-round in southern regions, and some inhabiting mid-latitude regions in summer and exhibiting relatively short- to moderate-distance migrations to and from winter ranges.

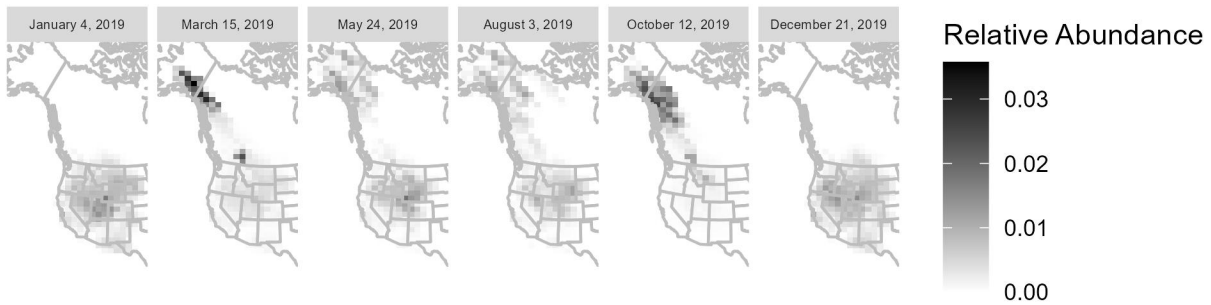


Figure 2: 2019 adaSTEM model output for Golden Eagles in Western North America that is used as our species distribution data for selected weeks. This highlights what we saw in the telemetry data that there are a range of migratory behaviors exhibited throughout individual golden eagles in the population.

We obtained locations of wind turbines in the U.S. from the U.S. Wind Turbine Database, provided by the U.S. Geological Survey, American Clean Power Association, and Lawrence Berkeley National Laboratory via <https://eerscmap.usgs.gov/uswtdb> (Hoen et al., 2016). These services provided locations of commercial wind turbines in the U.S., including characteristics of each such as year when first operational and size (in megawatts). We subset these data to the area of our species distribution data that is within the contiguous U.S., resulting in 18,456 wind turbines that are shown in Figure 3(a). Most turbines are close to

one another; because of this, we aggregated turbines to the 396 different wind projects that these 18,456 turbines comprise. A given wind project’s location was defined as the centroid of the locations of the wind turbines in that project. These wind project locations are displayed in Figure 3(b); it appears that wind project centroids are a reasonable surrogate for overall turbine distribution. We will consider wind project risk for golden eagles that winter in Utah County - Utah, Boulder County - Colorado, and Santa Fe County - New Mexico. These locations are shown in Figure 3(c).

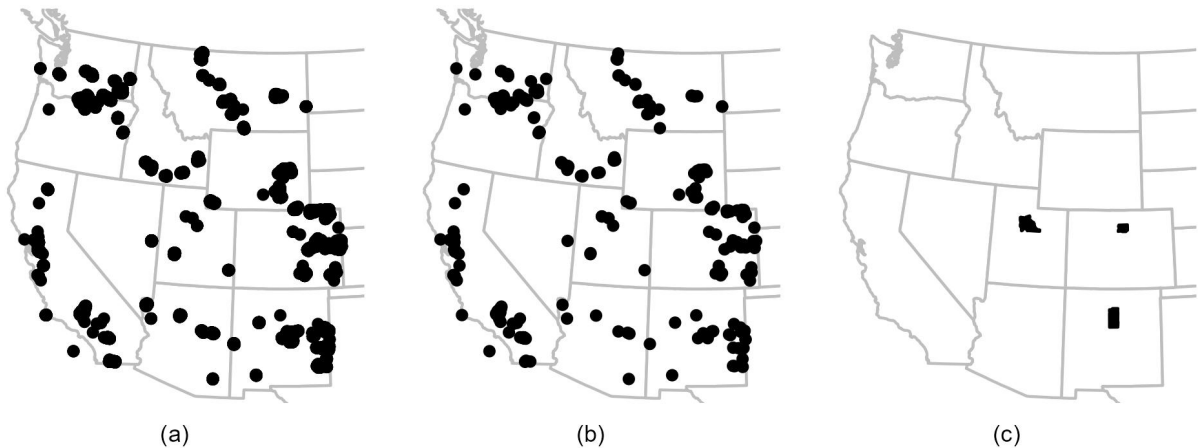


Figure 3: (a). Locations of the 18,456 wind turbines within the range of our species distribution data that is within the contiguous U.S.. (b). Locations of the 396 wind projects within the range of our species distribution data that is within the contiguous U.S.. (c). Locations of Utah County - Utah, Boulder County - Colorado, and Santa Fe County - New Mexico.

### 3 Methods

In this section, we describe our full annual cycle model for movement and population dynamics.

### 3.1 Integrated Movement Modeling

The IMM framework of Buderman et al. (2025) provides a formal approach for scaling individual level movement models to model population dynamics. First consider an individual movement model

$$x_{i,t+\Delta} \sim f(x_{i,t+\Delta}|x_{i,t}, \boldsymbol{\theta}_i, \boldsymbol{\psi}) \quad (1)$$

which defines the statistical distribution of  $x_{i,t+\Delta}$  which is the  $(x, y)$  position of the  $i^{\text{th}}$  animal at time  $t + \Delta$ . This model depends on where the animal was at time  $t$ , individual specific parameters  $\boldsymbol{\theta}_i$  and population parameters  $\boldsymbol{\psi}$ . We then specify a model,  $g$ , for how the parameters  $\boldsymbol{\theta}_i$  that govern individual movement vary across the population, given population parameters  $\boldsymbol{\psi}$

$$\boldsymbol{\theta}_i \sim g(\boldsymbol{\theta}_i|\boldsymbol{\psi}). \quad (2)$$

To obtain a model for the dynamics of the population, we specify an initial spatial distribution  $\pi_0(x)$ , where  $\pi_t(x)$  denotes the relative abundance of the population at location  $x$  at time  $t$ . We can then find  $\pi_t(x)$  by integrating over individual heterogeneity and the initial distribution

$$\pi_t(x) = \int \int f(x|z, \boldsymbol{\theta}_i, \boldsymbol{\psi}) g(\boldsymbol{\theta}_i|\boldsymbol{\psi}) \pi_0(z) d\boldsymbol{\theta}_i dz. \quad (3)$$

This double integral formulation provides us with a model for species distribution data with a formal link to the model used for individual tracking data. Buderman et al. (2025) show that likelihoods for population count data can be derived from an inhomogeneous Poisson point process with rates proportional to  $\pi_t(x)$ . Then for output from eBird status and trends adaSTEM model, which we will denote as  $sd_t(x)$ , Buderman et al. (2025) justify using a Poisson likelihood with

$$\tilde{sd}_t(x) \sim \text{Poisson}(K\pi_t(x)) \quad (4)$$

where  $\tilde{sd}_t(x) = \text{round}(K * sd_t(x))$  is a scaled version of the adaSTEM model output. The likelihoods in (1) and (4) define a joint model for telemetry data and species distribution

data. We use this general framework but improve upon Buderman et al. (2025) by modeling the full annual cycle, and deriving an analytic solution to the double integral, (3) for a SDE movement model.

### 3.2 Modeling Heterogeneity in Movement

Before presenting our time-varying OU model for movement and its scaling to population-level dynamics, it will be helpful to describe how we will model heterogeneity in movement behavior. We set our individual movement parameters to have a mixture model prior, replacing (2) with

$$g(\boldsymbol{\theta}_i|\boldsymbol{\psi}) = \sum_{p=1}^P \omega_{ip} g_p(\boldsymbol{\theta}_i|\boldsymbol{\psi}_p) \quad (5)$$

where  $\omega_{i1}, \dots, \omega_{iP}$  are nonnegative and sum to unity for each  $i$ . With the additional assumptions that we can partition  $\boldsymbol{\psi}$  into  $\boldsymbol{\psi}_1, \dots, \boldsymbol{\psi}_P$  such that  $g_p(\boldsymbol{\theta}_i|\boldsymbol{\psi}) = g_p(\boldsymbol{\theta}_i|\boldsymbol{\psi}_p)$  and that for each  $i$  one of the  $\omega_{ip} = 1$  and the rest are zero, this mixture model of variation in movement behavior is equivalent to having  $P$  sub-populations, each with their own parameters  $\boldsymbol{\psi}_p$ . We will define our model for movement by sub-population denoted by a superscript  $p$ .

### 3.3 A Time Varying OU Model For Full-Annual Cycle Individual Migratory Movement

We begin by defining our model for the individual tracking data of the eagles. We will use a time varying OU process to model the individual movement. OU processes have been used for modeling animal movement (Dunn and Gipson, 1977) as they can capture central place foraging behavior, and other common movement patterns. Blackwell (1997) introduced a time varying extension by considering a finite state continuous time Markov chain where each state corresponds to a different movement pattern (e.g. a OU process). Buderman et al. (2025) used an OU process for modeling spring migration of golden eagles, but only considered eight weeks of the year, used a time-homogenous SDE, and used a numerical

approximation to the SDE. We develop a much more general time-varying OU process model suitable for modeling the full annual cycle of migratory species, and show that a fully analytic solution is available, conditional only on the timing of the start of spring and fall migrations. As the general timing of migration is well studied for many migratory species, we propose an OU process model with a time-varying attractive point which controls when and where birds migrate as follows. Let  $\mathbf{x}_{i,t}^p$  denote the telemetry location at time  $t$  for bird  $i$  in sub-population  $p$ . We then propose a model for individual movement using the SDE

$$d\mathbf{x}_{i,t}^p = \begin{cases} -\theta^p(\mathbf{x}_{i,t}^p - \mathbf{m}_{iw}^p)dt + \sigma^p d\mathbf{W}_{i,t}^p & \text{if } t < b_{i1}^p \text{ or } t > b_{i2}^p \\ -\theta^p(\mathbf{x}_{i,t}^p - \mathbf{m}_{is}^p)dt + \sigma^p d\mathbf{W}_{i,t}^p & \text{if } b_{i1}^p < t < b_{i2}^p \end{cases}. \quad (6)$$

Here the drift term is the derivative of a quadratic potential function (Preisler et al., 2013; Russell et al., 2022; Eisenhauer et al., 2022) that is centered at a bird specific winter attractive point  $\mathbf{m}_{iw}^p$  and summer attractive point  $\mathbf{m}_{is}^p$  depending on the time of year. This model can also be seen as overdamped Langevin diffusion with a Gaussian stationary distribution that has a seasonally varying mean (Michelot, 2024). The bird specific migration timing parameters  $b_{i1}^p$  and  $b_{i2}^p$  correspond to when the bird starts migrating in the spring and fall, respectively. Under this model, mean movement is in the direction of the attractive points with random variation modeled through 2-dimensional Brownian motion ( $\mathbf{W}_{i,t}^p$ ). This model is a time varying OU process which has an exact solution (Gardiner, 2009), depending on the time interval and migration timing parameters:

$$\mathbf{x}_{i,t+\Delta}^p | \mathbf{x}_{i,t}^p \sim \mathcal{N} \left( \mathbf{x}_{i,t}^p e^{-\theta^p \Delta} + w_{i,t}^p(\Delta) \mathbf{m}_{iw}^p + s_{i,t}^p(\Delta) \mathbf{m}_{is}^p, \frac{(\sigma^p)^2}{2\theta^p} (1 - e^{-2\theta^p \Delta}) \mathbf{I} \right), \quad \Delta \leq 365 - t \quad (7)$$

where

$$s_{i,t}^p(\Delta) = 1 - e^{-\theta^p \Delta} - w_{i,t}^p(\Delta) \quad (8)$$

and

$$w_{i,t}^p(\Delta) = \begin{cases} 1 - e^{-\theta^p \Delta} & \text{if } t < t + \Delta \leq b_{i1}^p < b_{i2}^p \\ (1 - e^{-\theta^p(b_{i1}^p - t)}) e^{-\theta^p(t + \Delta - b_{i1}^p)} & \text{if } t < b_{i1}^p < t + \Delta < b_{i2}^p \\ 0 & \text{if } b_{i1}^p \leq t < t + \Delta \leq b_{i2}^p \\ 1 - e^{-\theta^p(t + \Delta - b_{i2}^p)} & \text{if } b_{i1}^p < t < b_{i2}^p < t + \Delta \\ 1 - e^{-\theta^p \Delta} & \text{if } b_{i1}^p < b_{i2}^p \leq t < t + \Delta \\ (1 - e^{-\theta^p(b_{i1}^p - t)}) e^{-\theta^p(t + \Delta - b_{i1}^p)} + (1 - e^{-\theta^p(t + \Delta - b_{i2}^p)}) & \text{if } t < b_{i1}^p < b_{i2}^p < t + \Delta \end{cases} \quad (9)$$

In this model, the conditional mean of a bird's location at time  $t + \Delta$  given where it was at time  $t$  is a weighted average of its location at time  $t$  ( $\mathbf{x}_{i,t}$ ), its winter attractive point ( $\mathbf{m}_{iw}^p$ ), and its summer attractive point ( $\mathbf{m}_{is}^p$ ), where  $w_{i,t}^p(\Delta)$  and  $s_{i,t}^p(\Delta)$  control the weights on the respective winter and summer attractive points. The six different cases in (9) characterize the behavior of the bird during the time window  $(t, t + \Delta)$ . In the first case of (9), the interval  $(t, t + \Delta)$  is completely before the bird starts its spring migration, and so the bird is attracted only to the winter center,  $\mathbf{m}_{iw}^p$ , with  $s_{it}(\Delta) = 0$  and  $w_{it}(\Delta) = 1 - e^{-\theta^p \Delta}$ . This is the classic result for time homogeneous OU processes (e.g. Gardiner, 2009). In the second case, the interval  $(t, t + \Delta)$  contains  $b_{i1}^p$ , when the bird starts its spring migration, and the movement is a composite of homogeneous movement centered around  $\mathbf{m}_{iw}^p$  for the interval  $(t, b_{i1}^p)$  followed by homogeneous movement centered around  $\mathbf{m}_{is}^p$  for the interval  $(b_{i1}^p, t + \Delta)$ . The remaining four cases are similar, with behavior being a composition of homogeneous movement between different breakpoints where behavior shifts with the start of spring and/or fall migrations. This model gives us a likelihood for each telemetry data point conditional on the most recent telemetry observation. For the initial location of bird  $i$  in sub-population  $p$ , we assume a priori

that

$$x_{i0}^p \sim \mathcal{N}\left(\mathbf{m}_{iw}^p, \frac{(\sigma^p)^2}{2\theta^p} \mathbf{I}\right) \quad (10)$$

which is the stationary distribution of the model described in (7) during the winter months when the OU process is centered at  $\mathbf{m}_{iw}^p$ . The individual movement model in (7)-(10) captures the full annual cycle of individual migratory behavior using an analytically tractable time varying OU model.

### 3.4 Modeling Heterogeneity in Movement Behavior

We now specify our model for heterogeneity in movement behavior of individuals within each sub-population. As mentioned above, each sub-population can also equivalently be thought of as a component of our mixture model for variation in movement behavior. We allow the attractive points for birds within a sub-population to vary according to a Gaussian distribution with different mean vectors and covariance matrices for the summer and winter attractive points

$$\mathbf{m}_{iw}^p \sim \mathcal{N}(\boldsymbol{\mu}_w^p, \boldsymbol{\Sigma}_w^p) \quad \mathbf{m}_{is}^p \sim \mathcal{N}(\boldsymbol{\mu}_s^p, \boldsymbol{\Sigma}_s^p). \quad (11)$$

Combining (7) and (11) with standard multivariate normal theory allows us to marginalize over the individual movement centers and our marginalized SDE model for individual movement is

$$\mathbf{x}_{i,t+\Delta}^p | \mathbf{x}_{i,t}^p \sim \mathcal{N}\left(\mathbf{x}_{i,t}^p e^{-\theta^p \Delta} + w_{i,t}^p(\Delta) \boldsymbol{\mu}_w^p + s_{i,t}^p(\Delta) \boldsymbol{\mu}_s^p, \frac{(\sigma^p)^2}{2\theta^p} (1 - e^{-2\theta^p \Delta}) \mathbf{I} + (w_{i,t}^p(\Delta))^2 \boldsymbol{\Sigma}_w^p + (s_{i,t}^p(\Delta))^2 \boldsymbol{\Sigma}_s^p\right). \quad (12)$$

In our inference below, we use the model described in (7) rather than (12) as our likelihood for the telemetry data. However, we present (12) as it is useful for motivating the initial species distribution of Section 3.5 and is an intermediate step for the resulting population

dynamics of Section 3.6. We allow each sub-population to begin their spring migration between February 15 (Julian day 46) and June 15 (Julian Day 166) and their fall migration between August 1 (Julian day 213) and November 30 (Julian Day 334) (Bedrosian et al., 2018). We then allow each bird within each sub-population to vary when they migrate, with migration timing following a scaled and shifted beta distribution with sub-population specific shape parameters.

$$b_{i1}^p = 120a_{i1}^p + 46 \qquad b_{i2}^p = 121a_{i2}^p + 213 \qquad (13)$$

$$a_{i1}^p \sim \text{Beta}(\alpha_1^p, \alpha_2^p) \qquad a_{i2}^p \sim \text{Beta}(\alpha_3^p, \alpha_4^p) \qquad (14)$$

Thus we have a hierarchal mixture-model style prior for our individual-specific parameters. This model allows for each individual bird to have different migratory behavior while still allowing us to scale up our individual SDE model to an SDE model for the species distribution.

### 3.5 Initial Species Distribution

In order to use the individual movement model (7) to inform the spatio-temporal dynamics of the species distribution following (3) we need to specify an initial spatial distribution for the species distribution. We set

$$\pi_0(\mathbf{x}) = \sum_{p=1}^4 \eta^p \pi_0^p(\mathbf{x}) \qquad (15)$$

where  $\boldsymbol{\eta} = \begin{bmatrix} \eta^1 & \eta^2 & \eta^3 & \eta^4 \end{bmatrix}^T$  is a vector of weights that sum to unity and  $\pi_0^p(\mathbf{x})$  is the initial distribution of the birds in sub-population  $p$ . We model  $\pi_0^p(\mathbf{x})$  as a Gaussian distribution based off of the stationary distribution of the SDE model defined in (12)

$$\pi_0^p(\mathbf{x}) = \Phi \left( \mathbf{x}; \boldsymbol{\mu}_w^p, \frac{(\sigma^p)^2}{2\theta^p} \mathbf{I} + \boldsymbol{\Sigma}_w^p \right). \qquad (16)$$

where  $\Phi(\mathbf{y}; \boldsymbol{\nu}, \mathbf{V})$  is the density of a bivariate Gaussian distribution with mean  $\boldsymbol{\nu}$  and variance-covariance matrix  $\mathbf{V}$  evaluated at  $\mathbf{y}$ .

### 3.6 Resulting Population Dynamics

By integrating over the model for variation in movement behavior, (11) and (14), and initial spatial distribution for the species distribution (15) we can scale up our above individual movement model (7) to a model for the spatio-temporal dynamics of the species distribution. Due to the Gaussian structure in our initial spatial distribution and our model for movement heterogeneity, we can perform this integration for each mixture component then take a weighted sum of the resulting dynamics. Following (3) we propose calculating for each sub-population

$$\pi_t^p(\mathbf{x}) = \int \int \int \int \int \left[ f(\mathbf{x}_{i,t}^p | \mathbf{x}_{i,0}^p = \mathbf{z}) g(\mathbf{m}_{iw}^p | \boldsymbol{\mu}_w^p, \boldsymbol{\Sigma}_w^p) g(\mathbf{m}_{is}^p | \boldsymbol{\mu}_s^p, \boldsymbol{\Sigma}_s^p) g(b_{i1}^p | \alpha_1^p, \alpha_2^p) g(b_{i2}^p | \alpha_3^p, \alpha_4^p) \pi_0^p(\mathbf{z}) \right] d\mathbf{m}_{iw}^p d\mathbf{m}_{is}^p db_{i1}^p db_{i2}^p d\mathbf{z}, \quad (17)$$

which is the marginal spatial distribution of mixture component  $p$  at time  $t$ , marginalizing over the variation in individual movement behavior and the initial spatial distribution of that mixture component. As  $f(\mathbf{x}_{i,t}^p | \mathbf{x}_{i,0}^p = \mathbf{z})$ ,  $g(\mathbf{m}_{iw}^p | \boldsymbol{\mu}_w^p, \boldsymbol{\Sigma}_w^p)$ ,  $g(\mathbf{m}_{is}^p | \boldsymbol{\mu}_s^p, \boldsymbol{\Sigma}_s^p)$ , and  $\pi_0^p(\mathbf{z})$  are all bivariate Gaussian distributions, if we assume that the migration timings ( $b_{i1}^p$  and  $b_{i2}^p$ ) are known, combining (12) and (16) with standard multivariate Gaussian distribution theory results in an analytic form for the spatial distribution for mixture component  $p$  at time  $t$ ,

$$\begin{aligned} \pi_t^p(\mathbf{x} | b_{i1}^p, b_{i2}^p) &= \int \int \int \left[ f(\mathbf{x}_{i,t}^p | \mathbf{x}_{i,0}^p = \mathbf{z}) g(\mathbf{m}_{iw}^p | \boldsymbol{\mu}_w^p, \boldsymbol{\Sigma}_w^p) g(\mathbf{m}_{is}^p | \boldsymbol{\mu}_s^p, \boldsymbol{\Sigma}_s^p) \pi_0^p(\mathbf{z}) \right] d\mathbf{m}_{iw}^p d\mathbf{m}_{is}^p d\mathbf{z} \\ &= \Phi \left( \mathbf{x}; (e^{-\theta^p t} + w_{i,0}^p(t)) \boldsymbol{\mu}_w^p + s_{i,0}^p(t) \boldsymbol{\mu}_s^p, \frac{(\sigma^p)^2}{2\theta^p} \mathbf{I} + (e^{-2\theta^p t} + [w_{i,0}^p(t)]^2) \boldsymbol{\Sigma}_w^p + [s_{i,0}^p(t)]^2 \boldsymbol{\Sigma}_s^p \right). \end{aligned} \quad (18)$$

Thus conditional on migration timing, we have an analytic Gaussian form for the spatio-temporal dynamics of a sub-population of animals that each move following our time-varying SDE model for full annual cycle migratory movement with mixture model variation in individual parameters. We cannot marginalize over the individual migration timings analytically in the same manner that we did with the individual migration attractive points. Instead, we propose to use quasi Monte-Carlo techniques (Morokoff and Caflisch, 1995) to approximate the solution to the marginalized distribution

$$\pi_t^p(\mathbf{x}) = \int \int \pi_t^p(\mathbf{x}|b_{i1}^p, b_{i2}^p) g(b_{i1}^p|\alpha_1^p, \alpha_2^p) g(b_{i2}^p|\alpha_3^p, \alpha_4^p) db_{i1}^p db_{i2}^p. \quad (19)$$

Denote this approximation as  $\tilde{\pi}_t^p(\mathbf{x})$ . To calculate this approximation we draw  $(a_{11}^{p*}, a_{12}^{p*})$ ,  $(a_{21}^{p*}, a_{22}^{p*})$ ,  $\dots$ ,  $(a_{Q1}^{p*}, a_{Q2}^{p*})$  from the Halton sequence (Halton, 1964) with base 2 for the first component and base 3 for the second component and calculate corresponding  $(b_{11}^{p*}, b_{12}^{p*})$ ,  $(b_{21}^{p*}, b_{22}^{p*})$ ,  $\dots$ ,  $(b_{Q1}^{p*}, b_{Q2}^{p*})$  by following (13). We use  $Q = 10$ . By using a low-discrepancy sequence, such as the Halton sequence, we consistently have a sample of design points that is dispersed on  $[0, 1] \times [0, 1]$  to capture the distribution systematically, with increasing precision as the number of points grows. Then we approximate the double integral with a quasi Monte-Carlo estimate based on our points drawn from the Halton sequence,

$$\tilde{\pi}_t^p(\mathbf{x}) = \sum_{q=1}^Q \pi_t^p(\mathbf{x}|b_{q1}^{p*}, b_{q2}^{p*}) \frac{g(b_{q1}^{p*}|\alpha_1^p, \alpha_2^p) g(b_{q2}^{p*}|\alpha_3^p, \alpha_4^p)}{\sum_{j=1}^Q g(b_{j1}^{p*}|\alpha_1^p, \alpha_2^p) g(b_{j2}^{p*}|\alpha_3^p, \alpha_4^p)}, \quad (20)$$

where  $g(b_{q1}^{p*}|\alpha_1^p, \alpha_2^p)$  and  $g(b_{q2}^{p*}|\alpha_3^p, \alpha_4^p)$  are the beta likelihoods of (14). We can then calculate the species distribution for the entire population of golden eagles by taking the weighted sum of the species distributions for each sub-population:

$$\pi_t(\mathbf{x}) = \sum_p \eta^p \tilde{\pi}_t^p(\mathbf{x}). \quad (21)$$

This analytic solution allows us to evaluate the population-level dynamics simply by evaluating bivariate Gaussian densities without needing to numerically solve any differential equations. Thus conducting inference which requires repeatedly evaluating the likelihood for the species distribution data (22) will be much faster than if we did not have an analytic solution and had to numerically approximate the solution to an SDE.

### 3.7 Species Distribution Likelihood

Let  $sd_t(\mathbf{x})$  be the observed species distribution output from the adaSTEM model (Fink et al., 2013) at location  $\mathbf{x}$  and time  $t$ . Then let  $\tilde{sd}_t(\mathbf{x}) = \text{round}(K * sd_t(\mathbf{x}))$  be a scaled version of this data. The Poisson likelihood (as justified in Buderman et al. (2025)),

$$\tilde{sd}_t(x) \sim \text{Poisson}(K\pi_t(x)), \quad (22)$$

is an appropriate likelihood for spatial species distribution data resulting from eBird adaSTEM model output. Based on estimates from the USFWS we fix  $K$ , a parameter that is interpretable as the total number of individuals in the geographic area of study, at 40,000 (U.S. Fish and Wildlife Service, 2016; Millsap et al., 2022).

### 3.8 Fitting The Model

The model that we fit is composed of (7), (10), (11),(14), and (22). For fitting the model we use a Bayesian approach and take draws from the posterior distribution. Thus, to fully specify our model we must specify priors for all parameters. For the sub-population attractiveness parameters and variances, which must be positive, we use diffuse log-normal priors

$$\theta^p \stackrel{iid}{\sim} \text{log-normal}(0, 10^{15}) \quad (23)$$

$$(\sigma^p)^2 \stackrel{iid}{\sim} \text{log-normal}(0, 10^{15}). \quad (24)$$

For means and variances of individual movement centers for each sub-population we use diffuse multivariate normal and Inverse-Wishart distributions

$$\boldsymbol{\mu}_w^p \stackrel{iid}{\sim} \mathcal{N}(\mathbf{0}, 10^{15}\mathbf{I}) \quad \boldsymbol{\Sigma}_w^p \stackrel{iid}{\sim} \text{Inverse Wishart}(3, \mathbf{I}) \quad (25)$$

$$\boldsymbol{\mu}_s^p \stackrel{iid}{\sim} \mathcal{N}(\mathbf{0}, 10^{15}\mathbf{I}) \quad \boldsymbol{\Sigma}_s^p \stackrel{iid}{\sim} \text{Inverse Wishart}(3, \mathbf{I}) \quad (26)$$

For the proportion of the species distribution in each sub-population we use a constrained Dirichlet distribution,

$$\boldsymbol{\eta} = 0.05\mathbf{1} + 0.8\boldsymbol{\eta}^* \quad (27)$$

$$\boldsymbol{\eta}^* \sim \text{Dirichlet}(\mathbf{1}). \quad (28)$$

This makes it so that each sub-population have at least 5% of the weight. To fit this model we use the Metropolis Hastings algorithm with the log adaptive tuning of Shaby and Wells (2010). We ran the MCMC sampler for 190,000 iterations which took about 100 hours. We assess convergence visually.

## 4 Results

In this section we present results from fitting the model specified in section 3 to the data described in section 2.

### 4.1 Golden Eagle Movement Dynamics

We first consider the movement dynamics of golden eagles in western North America. In Figure 4 the posterior mean of the fitted estimated relative abundance,  $\pi_t(\mathbf{x})$ , closely matches the data in Figure 2 showing the model's goodness of fit.

We show the posterior mean of the distribution of winter and summer attractive points,  $\mathbf{m}_{iw}^p$  and  $\mathbf{m}_{is}^p$ , in Figure 5. The posterior mean for the distributions of the timings of the

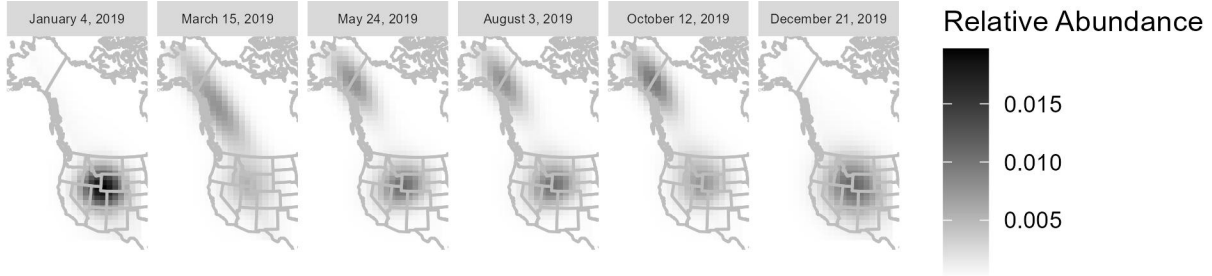


Figure 4: Posterior mean of the species distribution of Golden Eagles in western North America for specific weeks. This is comparable to the data which we have in Figure 2 showing the model’s goodness of fit.

spring and fall migration,  $b_{i1}^p$  and  $b_{i2}^p$ , with a 95% credible interval are shown in Figures 6 and 7. We see that while there is similarity in the distribution of the winter attractive points across sub-populations there is much more variation with the migration timings and the summer attractive point distribution. For example, sub-population one typically migrates to Canada and migrates during early spring and late fall; where sub-population three migrates slightly north to around Wyoming and migrates near the middle of the allowed window in both spring and fall.

## 4.2 Assessing Wind Project Risk

We now demonstrate use of this full-year probabilistic model for golden eagle distribution to assess wind project risk across time for eagles that winter in a specific location. The risk that wind projects pose to golden eagles is that of an eagle dying from collision with a turbine

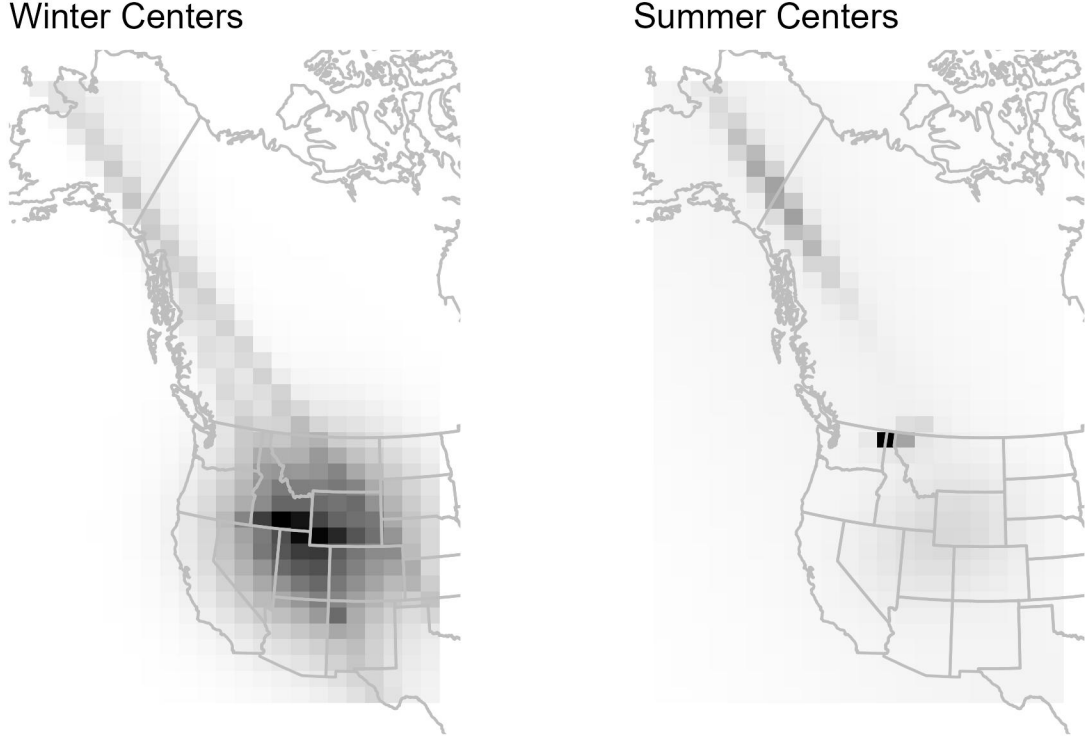


Figure 5: Posterior means of the distribution of winter and summer centers. Showing that in the winter the centers are more densely packed than in the summer.

(Beston et al., 2016; Gedir et al., 2025), specifically a turbine’s spinning blade (Hunt, 2002). However, throughout this section we will refer to the wind project risk, which is calculated as the probability of being within a square mile of the centroid of a wind projects, which is correlated with, and could be used as a proxy for, collision risk. We will consider wind project risk for eagles that winter in three counties in the western U.S.: Utah County - Utah, Boulder County - Colorado, and Santa Fe County - New Mexico. These three counties are shown in Figure 3(c). To estimate the spatio-temporal distribution for eagles wintering in a given location we fix the winter attractive points,  $\mathbf{m}_{iw}^p$ , for all four sub-populations as a point mass at the centroid of the county in question. We will call this value  $\mathbf{m}_w$ . We also set the initial spatial distribution of sub-population  $p$ ,  $\pi_0^p(\mathbf{x})$ , to be a point mass at  $\mathbf{m}_w$ . Let

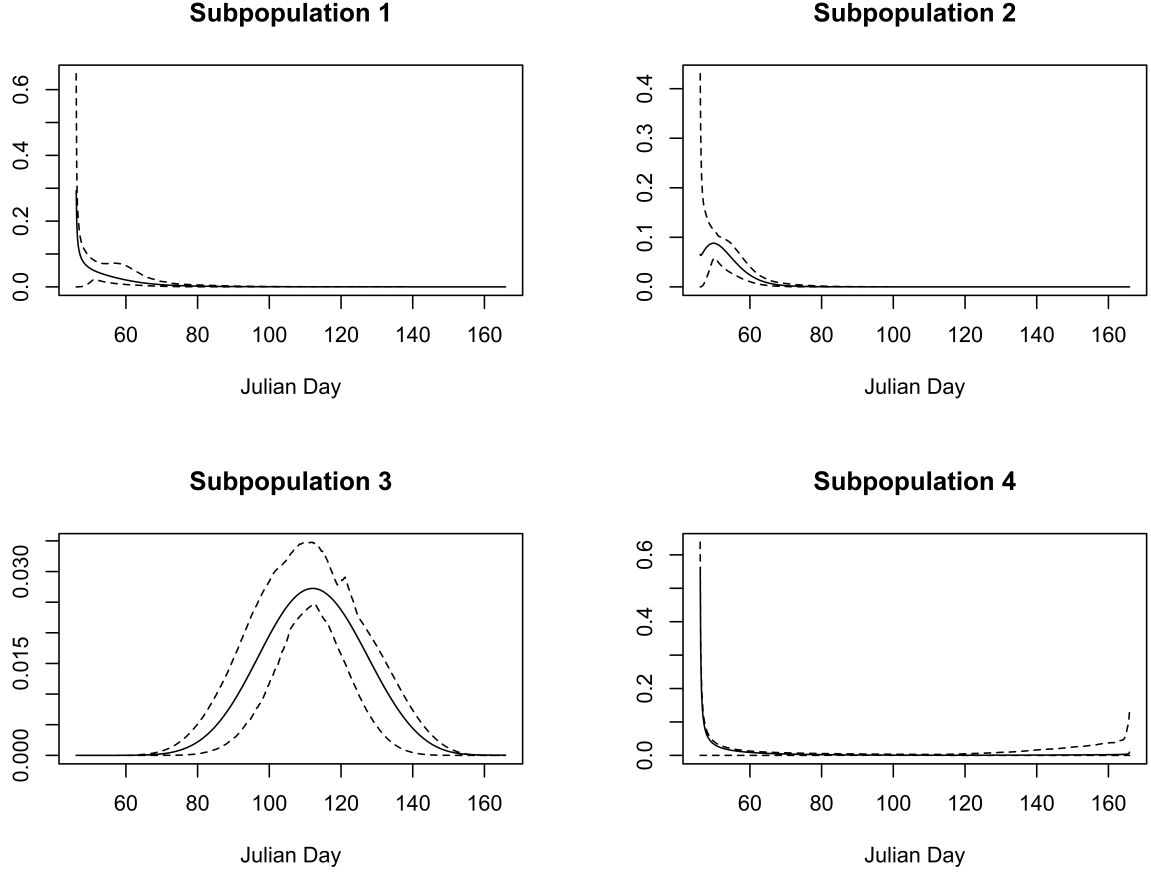


Figure 6: Posterior means and 95% credible intervals for the distribution of the onset of spring migration for each sub-population of golden eagles.

$\tilde{\xi}^p$  be the density value of the prior of  $\mathbf{m}_{iw}^p$ , given in (11), evaluated at  $\mathbf{m}_w$ . Then let

$$\xi^p = \frac{\tilde{\xi}^p}{\sum_{i=1}^4 \tilde{\xi}^p} \quad (29)$$

be the proportion of eagles at location  $\mathbf{m}_i$  who are from sub-population  $p$ . We then change our initial species distribution, given in (15), to

$$\pi_0(\mathbf{x}) = \sum_{p=1}^4 \xi^p \pi_0^p(\mathbf{x}). \quad (30)$$

This reflects an assumption that the proportion of individuals from a given sub-population at a certain location at the year's beginning is based solely on the distribution of the winter

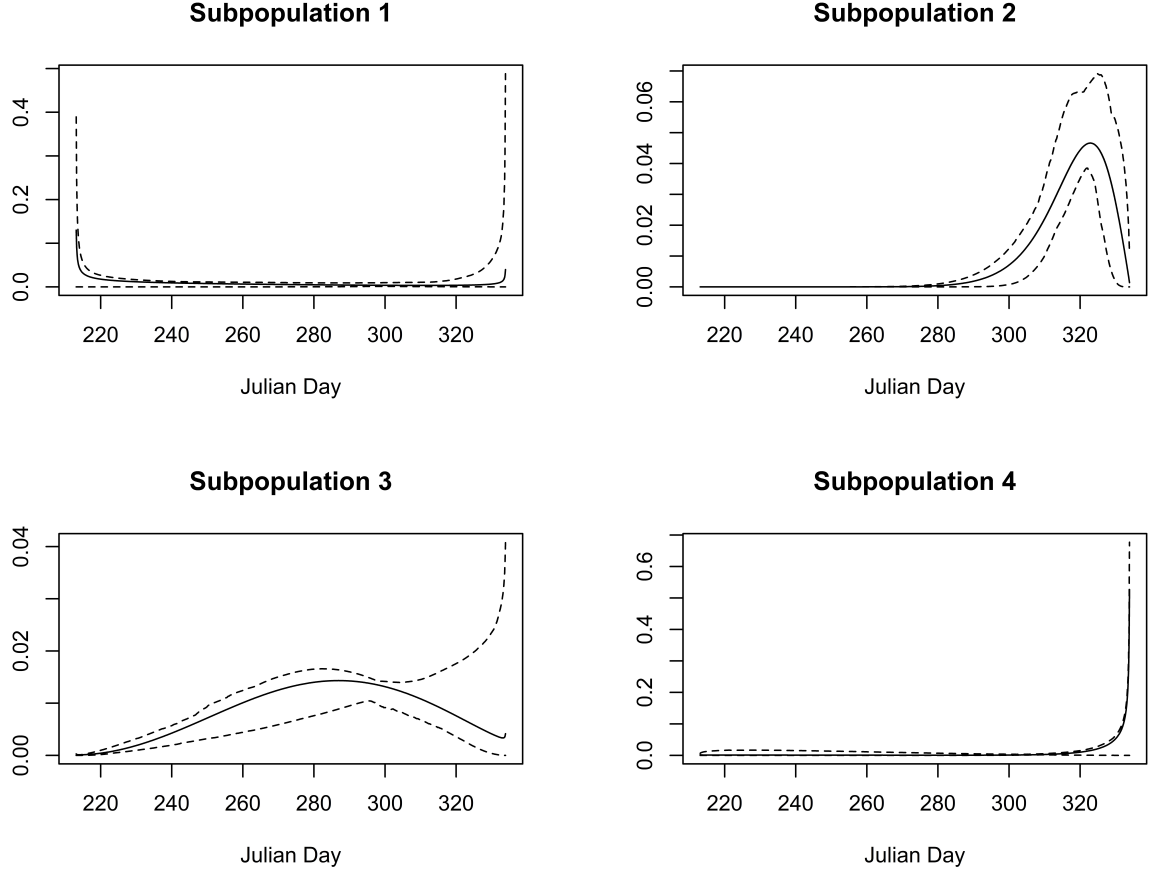


Figure 7: Posterior means and 95% credible intervals for the distribution of the onset of fall migration for each sub-population of golden eagles.

attractive points. These changes result in (18) becoming

$$\pi_t^p(\mathbf{x})|b_{i1}^p, b_{i2}^p \sim \mathcal{N}\left((e^{-\theta^p t} + w_{i,0}^p(t)) \mathbf{m}_w + s_{i,0}^p(t) \boldsymbol{\mu}_s^p, \frac{(\sigma^p)^2}{2\theta^p} (1 - e^{-2\theta^p t}) \mathbf{I} + [s_{i,0}^p(t)]^2 \boldsymbol{\Sigma}_s^p\right) \quad (31)$$

and (21) becoming

$$\pi_t(\mathbf{x}) = \sum_{p=1}^4 \xi^p \tilde{\pi}_t^p(\mathbf{x}). \quad (32)$$

All other results from the section 3.6 remain unchanged. Let  $P_{js}(t)$  be the probability that an eagle that winter in county  $j$  are within the 1 square mile centered at the centroid of wind project  $s$  which can be found by integrating by integrating  $\pi_t(\mathbf{x})$  over the relevant spatial

region. We estimate this integral for each  $\tilde{\pi}_t^p(\mathbf{x})$  using the algorithm of Donnelly (1973) and then take the weighted sum to obtain the integral of  $\pi_t(\mathbf{x})$ . We estimate the posterior mean of  $P_{js}(t)$  (hereafter called wind project risk) for each of the wind projects. We show these posterior means for our three different counties of interest in Figures 8(a)-(c). Let

$$Q_{js} = \int_0^{365} P_{js}(t) dt \quad (33)$$

be the occupancy time (Kulkarni, 2011): the mean number of days in a year that an eagle that winters in county  $j$  spends in the 1 square mile area centered at wind project  $s$ . Posterior means of  $Q_{js}$  for each wind project and each county are shown in Figures 8(d)-(f) with the 40 wind projects with the highest posterior mean occupancy time highlighted in red. We then show the location of these 40 wind projects in Figures 8(g)-(i) and the posterior mean wind project risk for these selected projects in Figures 8(j)-(l).

We see that for wind projects close to the county of interest, risk to eagles starts high, falls, and then increases again. For other wind projects we see relatively flat risk with spikes around the time when eagles wintering in each county migrate in the spring and fall. We also can see that wind projects that pose the greatest risk to eagles (as measured by posterior mean occupancy time) are those that are closest to the county of interest and those between the county of interest and Alaska. These results could help wildlife managers and wind energy proponents to understand and lessen the risks that golden eagles confront, or serve as integral components of a pre-construction environmental impact assessment.

## 5 Discussion

In this work we propose the first probabilistic full-year integrated movement model for jointly modeling individual tracking data and species distribution data. With this model we can answer questions about factors influencing a species distribution to various degrees at a given place and time such as the risk that certain wind projects pose to golden eagles that

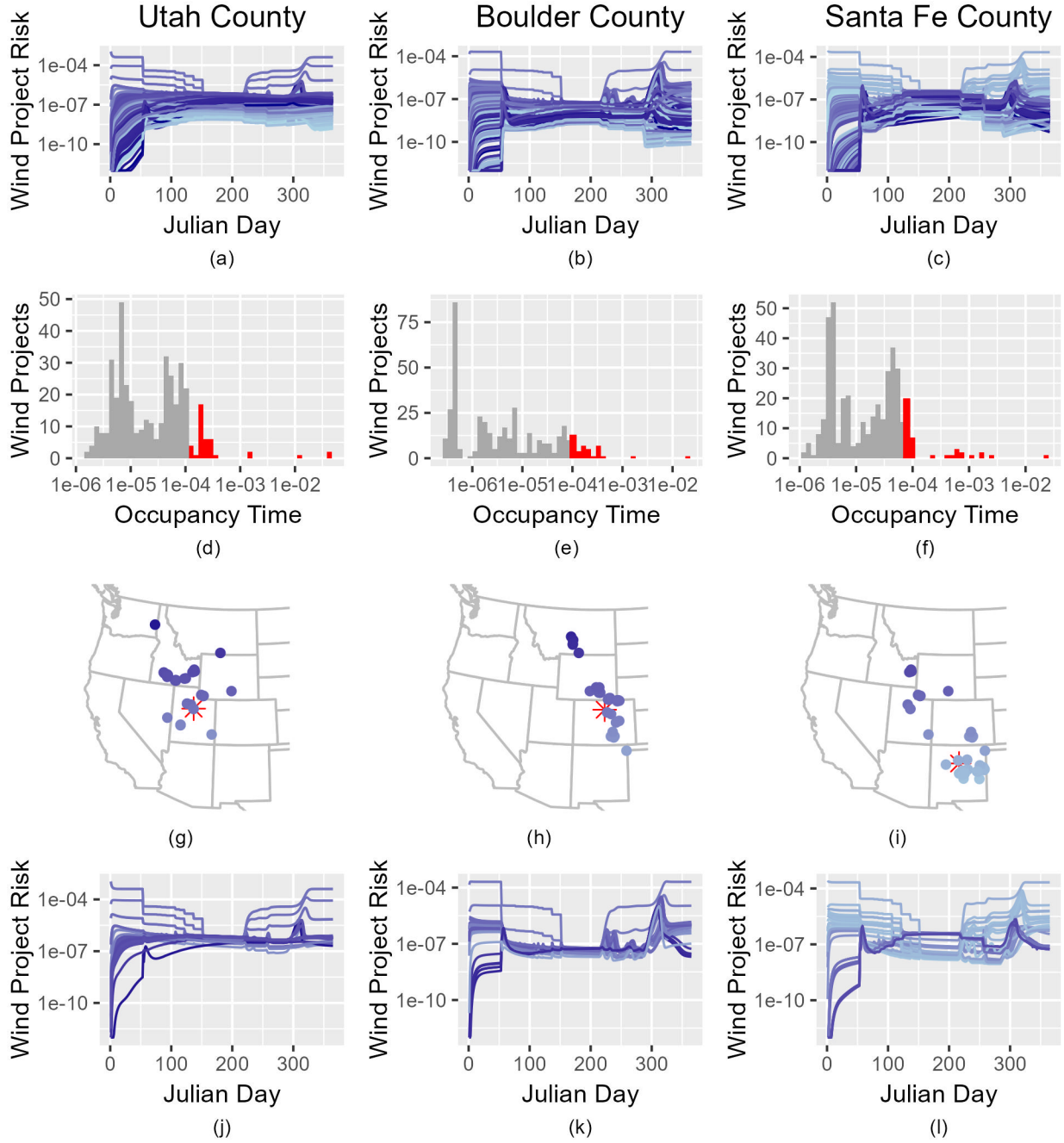


Figure 8: (a)-(c): Posterior mean wind project risk for each wind project across the year for golden eagles that winter in Utah, Boulder, and Santa Fe counties; colors correspond to latitudinal location of the wind project, with darker blue for more northerly projects. (d)-(f): Histogram of the posterior mean of occupancy time for each wind project; those wind projects with the greatest times are displayed in red ( $n = 40$  projects). (g)-(i): The 40 wind projects with the highest posterior mean occupancy time and the centroid of the county (the red asterisk). (j)-(l): Posterior mean wind project risk for the 40 wind projects with the highest posterior mean occupancy time across the year. The axes for wind project risk and occupancy time are on a logarithmic scale.

winter in specific locations. Such information could help support land use planning decisions that ultimately influence the conservation status of some migratory species of wildlife. Methods presented herein possibly could be used in environmental impact assessments. For golden eagles specifically, results from the model could be included in Eagle Conservation Plans that are recommended by the U.S. Fish and Wildlife Service “...to help make wind energy facilities compatible with eagle conservation and the laws and regulations that protect eagles” (U.S. Fish and Wildlife Service, 2013).

In this work we took an empirical Bayes approach and fixed each eagle to one mixture component at the start. We could instead allow each eagle’s individual telemetry data and parameters to follow a mixture model with no constraints on the weights. We could also increase the number of mixture components used to create a more flexible model, or use a Dirichlet process prior for a fully nonparametric model for heterogeneity in movement behavior.

In this work, we treat each year of an eagle’s telemetry data as independent. We could instead treat the tracking data of each eagle as a multiyear time series and adjust the model so we could perform inference on how the individual behavior changes over time. We could similarly use multiple years of species distribution data. Doing so would increase computation time approximately linearly.

The individual movement model utilized herein is flexible yet is simplistic in some ways. While this simplicity enabled efficient computation, it could be of interest to utilize a more realistic model for individual movement. Two of the parameters in our model,  $\sigma$  and  $\beta$ , have been shown to be linked to the speed at which an animal is moving (Michelot et al., 2019, 2021). We assume that these coefficients (and thus the speed at which the eagles move) is constant throughout the year. This is definitely not true of continental scale migratory species such as golden eagles who quickly switch from central place foraging behavior to migration across long distances. Extensions where we allow these parameters to vary across time, such as increasing  $\sigma$  during the period of migration, could be considered to improve

the fit of the model.

This work provides the first formal integration of full-year movement and species distribution data and provides a framework for studying spatio-temporal risk in migratory species at the continental scale.

## 6 Acknowledgments

Robert K. Murphy is per contract with the U.S. Fish & Wildlife Service—Division of Migratory Bird Management, National Raptor Program. We thank the eBird participants for their contributions, the eBird data management, and the U.S. Fish and Wildlife Service’s Division of Migratory Bird Management, National Raptor Program for providing the Golden eagle location data. We also acknowledge Viviana Ruiz-Gutierrez, whose insights helped frame this paper.

This material uses data from the eBird Status and Trends Project at the Cornell Lab of Ornithology, eBird.org. Any opinions, findings, and conclusions or recommendations expressed in this material are those of the authors and do not necessarily reflect the views of the Cornell Lab of Ornithology.

## 7 Funding

Michael L. Shull and Ephraim M. Hanks were supported by the National Science Foundation (DMS-2015273). Frances E. Buderman was supported by the U.S. Department of Agriculture National Institute of Food and Agriculture and Hatch Appropriations under Hatch Project #PEN04758 and Accession #1024904.

## 8 Disclosure Statement

The authors report there are no competing interests to declare

## References

- Bedrosian, B. E., Domenech, R., Shreading, A., Hayes, M. M., Booms, T. L., and Barger, C. R. (2018). Migration corridors of adult Golden Eagles originating in northwestern North America. *PloS one*, 13(11):e0205204.
- Beston, J. A., Diffendorfer, J. E., Loss, S. R., and Johnson, D. H. (2016). Prioritizing Avian Species for Their Risk of Population-Level Consequences from Wind Energy Development. *PloS one*, 11(3):e0150813.
- Blackwell, P. (1997). Random diffusion models for animal movement. *Ecological Modelling*, 100(1-3):87–102.
- Buderman, F. E., Hanks, E. M., Ruiz-Gutierrez, V., Shull, M., Murphy, R. K., and Miller, D. A. (2025). Integrated movement models for individual tracking and species distribution data. *Methods in Ecology and Evolution*, 16(2):345–361.
- Donnelly, T. G. (1973). Algorithm 462: Bivariate normal distribution. *Communications of the ACM*, 16(10):638.
- Dunn, J. E. and Gipson, P. S. (1977). Analysis of radio telemetry data in studies of home range. *Biometrics*, pages 85–101.
- Eisenhauer, E., Hanks, E., Beckman, M., Murphy, R., Miller, T., and Katzner, T. (2022). A flexible movement model for partially migrating species. *Spatial Statistics*, 50:100637.
- Fink, D., Auer, T., Johnston, A., Strimas-Mackey, M., Robinson, O., Ligocki, S., Hochachka, W., Jaromczyk, L., Wood, C., Davies, I., Iliff, M., and Seitz, L. (2021). <https://science.ebird.org/en/status-and-trends> (2021) eBird Status and Trends, Data Version: 2020. eBird Status and Trends, Data Version: 2020.
- Fink, D., Damoulas, T., Bruns, N. E., La Sorte, F. A., Hochachka, W. M., Gomes, C. P.,

- and Kelling, S. (2014). Crowdsourcing meets ecology: hemisphere-wide spatiotemporal species distribution models. *AI magazine*, 35(2):19–30.
- Fink, D., Damoulas, T., and Dave, J. (2013). Adaptive Spatio-Temporal Exploratory Models: Hemisphere-wide species distributions from massively crowdsourced eBird data. In *Proceedings of the AAAI Conference on Artificial Intelligence*, volume 27, pages 1284–1290.
- Gardiner, C. (2009). Markov Processes. In *Stochastic Methods*, pages 42–76. Springer.
- Gedir, J. V., Gould, M. J., Millsap, B. A., Howell, P. E., Zimmerman, G. S., Bjerre, E. R., and White, H. M. (2025). Estimated golden eagle mortality from wind turbines in the western United States. *Biological Conservation*, 302:110961.
- Gow, E. A., Knight, S. M., Bradley, D. W., Clark, R. G., Winkler, D. W., Bélisle, M., Berzins, L. L., Blake, T., Bridge, E. S., Burke, L., et al. (2019). Effects of spring migration distance on tree swallow reproductive success within and among flyways. *Frontiers in Ecology and Evolution*, 7:380.
- Halton, J. H. (1964). Algorithm 247: Radical-inverse quasi-random point sequence. *Communications of the ACM*, 7(12):701–702.
- Hertel, A. G., Niemelä, P. T., Dingemanse, N. J., and Mueller, T. (2020). A guide for studying among-individual behavioral variation from movement data in the wild. *Movement Ecology*, 8:1–18.
- Hoen, B., Diffendorfer, J., Rand, J., Kramer, L., Garrity, C., and Hunt, H. (2016). United States Wind Turbine Database v7.1 (August 14, 2024): U.S. Geological Survey, American Clean Power Association, and Lawrence Berkeley National Laboratory data release, <https://doi.org/10.5066/F7TX3DN0>.

- Howell, P. E., Devers, P. K., Robinson, O. J., and Royle, J. A. (2022). Leveraging community science data for population assessments during a pandemic. *Ecological Applications*, 32(3):e2529.
- Hunt, G. W. (2002). Golden Eagles In A Perilous Landscape: Predicting The Effects Of Mitigation For Wind Turbine Blade-Strike Mortality. Public Interest Energy Research, California Energy Commission, Sacramento, California, U.S.
- Hunt, G. W. and Watson, J. W. (2016). Addressing the factors that juxtapose raptors and wind turbines. *Journal of Raptor Research*, 50(1):92–96.
- Kulkarni, V. G. (2011). *Introduction to modeling and analysis of stochastic systems*, volume 1. Springer, 2nd edition.
- Michelot, T. (2024). Multiscale modelling of animal movement with persistent dynamics. *arXiv preprint arXiv:2406.15195*.
- Michelot, T., Glennie, R., Harris, C., and Thomas, L. (2021). Varying-coefficient stochastic differential equations with applications in ecology. *Journal of Agricultural, Biological and Environmental Statistics*, 26:446–463.
- Michelot, T., Gloaguen, P., Blackwell, P. G., and Étienne, M.-P. (2019). The Langevin diffusion as a continuous-time model of animal movement and habitat selection. *Methods in ecology and evolution*, 10(11):1894–1907.
- Millsap, B. A., Zimmerman, G. S., Kendall, W. L., Barnes, J. G., Braham, M. A., Bedrosian, B. E., Bell, D. A., Bloom, P. H., Crandall, R. H., Domenech, R., et al. (2022). Age-specific survival rates, causes of death, and allowable take of golden eagles in the western United States. *Ecological Applications*, 32(3):e2544.
- Morokoff, W. J. and Caflisch, R. E. (1995). Quasi-monte carlo integration. *Journal of Computational Physics*, 122(2):218–230.

- Murphy, R. K., Dunk, J. R., Woodbridge, B., Stahlecker, D. W., LaPlante, D. W., Millsap, B. A., and Jacobson, K. V. (2017). First-year dispersal of Golden Eagles from natal areas in the southwestern United States and implications for second-year settling. *Journal of Raptor Research*, 51(3):216–233.
- Murphy, R. K., Stahlecker, D. W., Millsap, B. A., Jacobson, K. V., Johnson, A., Smith, C. S., Tator, K. J., and Kruse, K. L. (2019). Natal dispersal distance of Golden Eagles in the southwestern United States. *Journal of Fish and Wildlife Management*, 10(1):213–218.
- Norevik, G., Åkesson, S., and Hedenström, A. (2025). The spatial consistency and repeatability of migratory flight routes and stationary sites of individual European nightjars based on multiannual GPS tracks. *Movement Ecology*, 13(1):8.
- Preisler, H. K., Ager, A. A., and Wisdom, M. J. (2013). Analyzing animal movement patterns using potential functions. *Ecosphere*, 4(3):1–13.
- Ruiz-Gutierrez, V., Bjerre, E. R., Otto, M. C., Zimmerman, G. S., Millsap, B. A., Fink, D., Stuber, E. F., Strimas-Mackey, M., and Robinson, O. J. (2021). A pathway for citizen science data to inform policy: A case study using eBird data for defining low-risk collision areas for wind energy development. *Journal of Applied Ecology*, 58(6):1104–1111.
- Russell, J. C., Hanks, E. M., Haran, M., and Hughes, D. (2022). A spatially varying stochastic differential equation model for animal movement. *Annals of Applied Statistics*, 12:1312–1331.
- Shaby, B. and Wells, M. T. (2010). Exploring an adaptive Metropolis algorithm. *Duke Technical Report*.
- Steinley, D. (2006). K-means clustering: a half-century synthesis. *British Journal of Mathematical and Statistical Psychology*, 59(1):1–34.

- Stillman, A. N., Howell, P. E., Zimmerman, G. S., Bjerre, E. R., Millsap, B. A., Robinson, O. J., Fink, D., Stuber, E. F., and Ruiz-Gutierrez, V. (2023). Leveraging the strengths of citizen science and structured surveys to achieve scalable inference on population size. *Journal of Applied Ecology*, 60(11):2389–2399.
- Stuber, E. F., Robinson, O. J., Bjerre, E. R., Otto, M. C., Millsap, B. A., Zimmerman, G. S., Brasher, M. G., Ringelman, K. M., Fournier, A. M., Yetter, A., et al. (2022). The potential of semi-structured citizen science data as a supplement for conservation decision-making: Validating the performance of eBird against targeted avian monitoring efforts. *Biological Conservation*, 270:109556.
- U.S. Department of the Interior (2024). North American Waterfowl Management Plan Update: Expanding the Partnership. U.S. Department of the Interior, Washington D.C., U.S..
- U.S. Fish and Wildlife Service (2013). Eagle Conservation Plan Guidance. Module 1 – Land-based Wind Energy, version 2. U.S. Fish and Wildlife Service, Division of Migratory Bird Management, Washington D.C., U.S..
- U.S. Fish and Wildlife Service (2016). Bald and Golden Eagles: Population demographics and estimation of sustainable take in the United States, 2016 update. U.S. Fish and Wildlife Service, Division of Migratory Bird Management, Washington D.C., U.S..